MOEM

Modern Electronic Materials 2020; 6(1): 1–7
DOI 10.3897/j.moem.6.1.53248

Research Article

Potential of using inert gas flows for controlling the quality of as-grown silicon single crystal

Tatyana V. Kritskaya[1], Vladimir N. Zhuravlev[2], Vladimir S. Berdnikov[3]

1 *Engineering Institute of Zaporizhzhya National University, 226 Soborny Ave., Zaporizhzhia 69006, Ukraine*

2 *Zaporozhye Machine-Building Design Bureau Progress State Enterprise named after Academician A.G. Ivchenko, 2 Ivanova Str., Zaporizhzhia 69068, Ukraine*

3 *Kutateladze Institute of Thermophysics, Siberian Branch of the Russian Academy of Sciences, 1 Academician Lavrentieva Ave., Novosibirsk 630090, Russia*

Corresponding author: Tatyana V. Kritskaya (krytskaja2017@gmail.com)

Received 30 October 2019 ♦ **Accepted** 23 November 2019 ♦ **Published** 30 March 2020

Citation: Kritskaya TV, Zhuravlev VN, Berdnikov VS (2020) Potential of using inert gas flows for controlling the quality of as-grown silicon single crystal. Modern Electronic Materials 6(1): 1–7. https://doi.org/10.3897/j.moem.6.1.53248

Abstract

We have improved the well-known Czochralski single crystal silicon growth method by using two argon gas flows. One flow is the main one (15–20 nl/min) and is directed from top to bottom along the growing single crystal. This flow entrains reaction products of melt and quartz crucible (mainly SiO), removes them from the growth chamber through a port in the bottom of the chamber and provides for the growth of dislocation-free single crystals from large weight charge. Similar processes are well known and have been generally used since the 1970s world over. The second additional gas flow (1.5–2 nl/min) is directed at a 45 arc deg angle to the melt surface in the form of jets emitted from circularly arranged nozzles. This second gas flow initiates the formation of a turbulent melt flow region which separates the crystallization front from oxygen-rich convective flows and accelerates carbon evaporation from the melt. It has been confirmed that oxygen evaporated from the melt (in the form of SiO) acts as transport agent for nonvolatile carbon. Commercial process implementation has shown that carbon content in as-grown single crystals can be reduced to below the carbon content in the charge. Single crystals grown with two argon gas flows have also proven to have highly macro- and micro-homogeneous oxygen distributions, with much greater lengths of single crystal portions in which the oxygen concentration is constant and below the preset limit. Carbon contents of 5–10 times lower than carbon content in the charge can be achieved with low argon gas consumption per one growth process (15–20 nl/min *vs* 50–80 nl/min for conventional processes). The use of an additional argon gas flow with a 10 times lower flowrate than that of the main flow does not distort the pattern of main (axial) flow circumvention around single crystal surface, does not hamper the "dislocation-free growth" of crystals and does not increase the density of microdefects. This suggests that the new method does not change temperature gradients and does not produce thermal shocks that may generate thermal stresses in single crystals.

Keywords

Czochralski method, silicon melt, single crystal, argon gas, main flow, additional flow, homogeneity, oxygen, carbon.

1. Introduction

Structural perfection of single crystal silicon (absence of grain boundaries, dislocations and associations of vacancies or interstitial atoms and their low bulk distribution density) and homogeneous distribution of doping impurities and background impurities are the main quality parameters of single crystals that determine their applicability for microelectronics, high-power electronics and solar engineering. Homogeneity of doping impurity distributions is typically assessed from the difference of the electrical resistivity from the preset one at distances of within several fractions of a micrometer or within several decades of centimeters along or across single crystals. The distributions of background impurities (oxygen and carbon) are usually evaluated based on changes in background impurity concentrations as determined by IR absorption methods. Optically active oxygen and carbon concentrations are characterized from the most intense absorption bands at 1106 and ~607 cm^{-1}, respectively [ASTM F 1188, F 1391].

Until recently the semiconductor industry was completely satisfied with Czochralski grown silicon single crystals (Cz-Si) having dislocation densities of less than 10 cm^{-2}, a radial doping impurity distribution inhomogeneity of 7–15% and an oxygen content (N_O) of within (5–9) × 10^{17} cm^{-3}. However the development of submicron integrated circuits (IC) and the transition to nanoscale IC technologies impose rapidly growing requirements to the quality of dislocation-free silicon single crystals. For example the radial scatter of electrical resistivity should be within ±5% and the oxygen concentration should vary along the crystal length within (8 ± 1) × 10^{17} cm^{-3} or (7 ± 0.5) × 10^{17} cm^{-3}. The carbon concentration N_C should be within (0.5–1.0) × 10^{16} cm^{-3} and the concentration of metallic impurities (iron) should not exceed 1 × 10^{10} cm^{-3}. The distribution and density of point microdefects depend largely on the distribution and concentration of impurities and the intensity of their mutual interactions during the growth and subsequent heat treatment of single crystals. The sizes and distribution density of the microdefects should be limited to 0.06–0.07 μm and 0.12–0.13 cm^{-2}, respectively [1, 2].

The above requirements are imposed by IC processes, e.g. gettering, high-resolution lithography, synthesis of a continuous gate oxide layer with good dielectric properties etc. [2, 3–11].

The continuous improvement of the Czochralski growth technique over the last 50 years has had several milestones toward axial and radial inhomogeneity elimination:

– various options of melt feeding with solid and liquid phases (the double-crucible and floating crucible methods [12–15]);
– regular stirring of established flows in the melt (short-time crucible rotation interruptions [16–18]);
– intentional deformation of the capillary column under the melt [5, 19];
– control of convective flows in the melt with programmable crystal and crucible rotation speed [20–25].

Since recently large diameter single crystals (200+ mm) have been grown with the application of magnetic fields for suppressing free convection and altering mass transport mechanisms in the melt. Oxygen concentrations achieved using this approach may vary over a wide range, from (4–5) × 10^{17} to (9–18) × 10^{17} cm^{-3} [26–30].

The major objective of all the abovementioned approaches is to reduce the inhomogeneity of doping impurity distributions, the most recent methods further aiming at an improvement of the axial oxygen distribution in single crystals [31–34]. However simultaneous achievement of high axial and radial homogeneity of doping impurity and oxygen distributions proved to be a complex task and therefore not all of these methods have been implemented commercially. Furthermore single crystal growth techniques incorporating the abovementioned methods could not improve the distribution and concentration of carbon in single crystals. Carbon concentration was successfully reduced by increasing the inert gas flow circumventing the growing crystal and more intense inert gas removal from the growth chamber.

The aim of this work is to analyze the possibility of establishing convective flows in silicon melt aiming at achieving a homogeneous bulk distribution of doping impurity (oxygen) and reducing the carbon content.

2. Experimental

In the investigation reported herein we made allowance for the fact that the pressure and dynamics of inert gas flows in the growth chamber may significantly affect the distribution and concentration of oxygen in the single crystal [35, 36]. For example if the single crystal is grown at a low pressure in the growth chamber (0.13–0.76 kPa) and an argon gas flowrate of >15 nl/min [1] the distribution of oxygen in the single crystal is homogeneous and the oxygen concentration N_O is close to those for single crystals grown in deep vacuum. A homogeneous oxygen distribution along the crystal is provided for by the fact that the radial profiles of the widths of the dynamic and diffusion boundary layers above the surface remain almost unchanged throughout the entire growth process, i.e., single crystals grow at a constant SiO evaporation rate. However this growth setup limits the potential for N_O adjustment aimed at achieving the optimum oxygen concentration for IC fabrication (8 × 10^{17} cm^{-3}) and makes such adjustment quite resource-consuming (high argon consumption, gas removal system upgrading costs etc.).

Analysis of different melt flow modes in the vicinity of the three-phase interface (crystallization front / melt / gas phase) revealed a nonuniform melt flowrate distribution, possibility of melt flow “slipping” along the crystal and hence crystal depletion of the impurity in regions close to the side surface [37, 38]. Supply of oxygen-rich molten silicon from the crucible surface to the sub-crystal region

occurs by melt flowing under the melt surface between the crucible wall and the growing crystal. Oxygen in the form of SiO is evaporated intensely as it reaches the melt surface since it is a volatile impurity. The evaporation rate is the highest at the crucible wall and decreases approaching the sub-crystal region. The melt flow mode formed by natural convection and crucible rotation provides for N_O reduction in the crystal but causes a large radial scatter of N_O.

Carbon in silicon melt is a low-volatile impurity [38, 39], the limiting evaporation stage being the surface kinetics:

$$\alpha = \gamma G\left(\frac{kT}{2\pi m}\right)^{1/2}, \quad (1)$$

where α is the kinetic evaporation coefficient, γ is the accommodation coefficient (probability that a molecule incident on the surface is not reflected), G is the distribution coefficient between the gas and liquid phases and m is the molecular weight.

Since carbon is predominantly evaporated from the melt in the form of CO its volatility is determined by the concentration and evaporation conditions of the highly volatile oxygen impurity:

$$\alpha' = \left(\frac{4Df}{\pi L}\right)^{1/2}, \quad (2)$$

where α' is the diffusion-convective evaporation coefficient, D is the impurity diffusion coefficient in the melt, f is the flowrate of the convective flow ascending from the melt and moving along its surface and L is the linear dimension of the melt surface. (Equations (1) and (2) are provided here to describe the important factors that affect the evaporation kinetics (diffusion-convective evaporation coefficient, carbon diffusion coefficient in the melt, convective flowrate for evaporation to vacuum, dimension of melt surface from which impurity is evaporated etc.), adjusting which one can control carbon evaporation.)

The equilibrium vapor phase above the melt mainly contains molecular silicon and carbon monoxides (SiO and CO). However in practice the partial pressure of Co is far lower than that of SiO because the carbon concentration in semiconductor purity silicon melts is always lower than its concentration in saturated vapor (~3×10^{18} cm^{-3}). The surface concentration of the highly volatile oxygen impurity is far lower than its concentration in the silicon melt bulk. The partial pressure of CO is proportional to the low surface concentration of oxygen and this in fact leads to the low carbon evaporation rate. Thus using an inert gas flow in combination with intentionally induced convective flows in the melt one can achieve high radial and axial homogeneity of impurity distributions (oxygen, doping impurities and carbon) and accelerate carbon evaporation from the melt.

Silicon single crystals were grown on Redmet-30 commercial growth plants. The properties of the as-grown silicon single crystals were improved by additionally blowing the melt surface with a specially directed argon gas flow [40]. Conventional heating units for 330 mm crucibles installed in growth plants were used.

By way of example of single crystal growth process implementation we describe the growth of a 100 mm diam. single crystal from a 330 mm crucible with a 22 kg charge.

We used a graphite resistive heater in the form of a regular 360 mm prism with a resistivity of 0.028–0.03 Ohm × cm. The power consumption of the heater was 48 kVA in the beginning of growth and 52 kVA at the end. Argon gas was supplied from the top of the growth chamber and removed through a port in the bottom of the chamber. The chamber pressure during the growth was maintained at 10 mm Hg (1.33 kPa). The argon gas flow was directed from top to bottom along the growing single crystal, the flowrate being 15–20 nl/min. The crucible with bulk-loaded silicon charge was installed onto a graphite pad inside the heater, the chamber was evacuated, argon gas was supplied and charge melting started. After complete melting of the silicon charge a special device with refractory nozzles for additional argon gas jet supply was brought to the melt surface. The nozzle orifices were 0.8 mm in diameter, the argon gas flowrate being 1.5–2.0 nl/min. The argon gas jets were directed at a 45 arc deg angle to the melt surface and were circularly arranged over the middle part of the open melt surface between the growing single crystal and the crucible walls. The distance between the nozzle orifice and the melt surface was kept at 10–15 mm throughout the entire growth process. The crystal and the crucible rotated in the opposite directions at the speeds ω_{sc} = 12–15 rpm and ω_c = 3–5 rpm, respectively.

The use of an additional argon gas flow with a 10 times lower flowrate than that of the main flow does not distort the pattern of main (axial) flow circumvention around single crystal surface, does not hamper the "dislocation-free growth" of crystals and does not increase the density of microdefects. This suggests that the new method does not change temperature gradients and does not produce thermal shocks that may generate thermal stresses in single crystals.

Figure 1 shows schematic diagram of the plant for single crystal growth in an argon gas flow for the implementation of the process designed herein.

Argon gas is supplied from multiple (up to seven) circularly arranged equally spaced nozzles. The dislocation-free crystals grew in steady state mode. The preset single crystal diameter was maintained by keeping a constant melt level in the crucible relative to the crucible top edge. The process ended by growing the inverse cone. The melt remainder in the crucible after growth completion was ~7–10% of the charge weight.

3. Results and discussion

The as-grown single crystals had high homogeneity of impurity distributions both in length and in cross-section. We could control the rated values of N_O and the oxygen axial distribution pattern by varying the number of nozzles.

Table 1 summarizes typical oxygen (N_O) and carbon (N_C) concentrations and the electrical resistivities of the

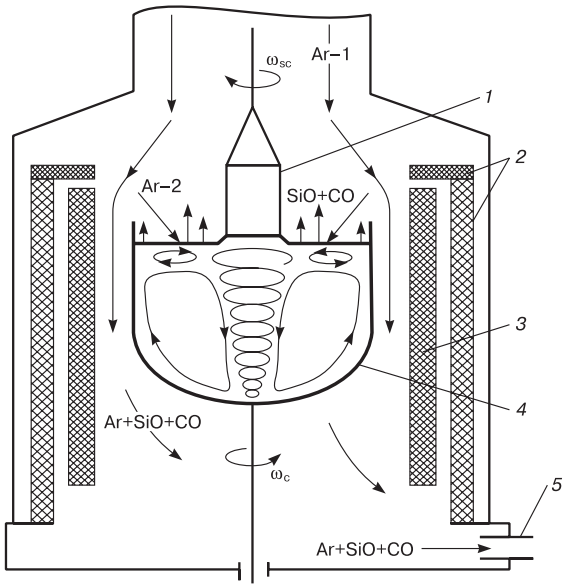

Figure 1. Schematic of single crystal growth in inert gas flow: (*1*) growing single crystal, (*2*) heat screens, (*3*) resistive heater, (*4*) crucible with silicon melt, (*5*) growth chamber gas removal port, Ar-1 argon gas flow circumventing the growing crystal (15–20 nl/min), Ar-2 argon gas flow in the form of jets (1.5–2.0 nl/min)

as-grown 100 mm diam. boron doped silicon single crystals (Grade 1A2yaO_2 KDB-10/2.5-102.5, charge weight 22 kg). The silicon single crystals were grown using three process variants:

- Variant 1 (V1): conventional growth method in an inert gas flow, ω_{sc} = 15 rpm, ω_c = 5 rpm, pulling rate 0.8–1.2 mm/min, linear programmable pulling rate variation;
- Variant 2 (V2): growth with programmable ω_c variation in accordance with earlier works [20, 41];
- Variant 3 (V3): new method with melt surface argon gas blowing from four nozzles [40,42].

Table 1. Typical parameters of single crystals grown using three process variants.

Crystal region	$N_O \cdot 10^{-18}$, cm^{-3}			$N_C \cdot 10^{-16}$, cm^{-3}			ER, Ohm·cm		
	V1	V2	V3	V1	V2	V3	V1	V2	V3
Top (20 mm):									
Center	1.1	0.95	0.92	4.0	3.8	0.7	12.2	12.0	11.6
Periphery	0.93	0.9	0.9	3.6	4.0	0.8	11.5	11.7	11.4
Middle (300–320 mm):									
Center	0.82	0.81	0.81	5.0	5.1	1.2	10.2	9.8	10.5
Periphery	0.72	0.78	0.78	5.1	4.6	1.1	9.8	9.4	10.3
Bottom									
Center	0.63	0.66	0.71	12.0	13.0	1.7	7.3	7.5	8.6
Center	0.56	0.58	0.68	11.0	11.0	1.5	6.9	6.8	8.3
Periphery									

The oxygen concentration was determined using a calibration factor equal to 2.45×10^{17} cm^{-2}.

The data on N_O, N_C and the electrical resistivities (Table 1) are given for three sections in the length of the single crystals with references to the distances (in mm) from the constant single crystal diameter establishment point. N_O and N_C were measured for cross-sections of specimens without process heat treatment (for thermodonor removal) and the electrical resistivities were measured after heat treatment (650 °C, 30 min). Single crystal growth using the method designed herein provides for a more homogeneous electrical resistivity distribution both in the length and in the cross-sections of the single crystals.

The data on N_O, N_C are given for the central and the peripheral regions of the specimen cross-sections, and the electrical resistivities are averaged over six measurement points along the cross-sections. To better illustrate the longitudinal and cross-sectional N_C distributions in the single crystal, we used silicon charge with N_C = (0.9–1.2) × 10^{17} cm^{-3} for all the three variants.

Table 1 shows that melt surface blowing with argon gas allows reducing N_C by several times to below the charge N_C value.

The designed method provides for a considerably more homogeneous oxygen distribution in the cross-section and length of the single crystals in comparison with the other two growth process variants. For example, the programmable ω_c variation method [20, 41] yields a greater radial inhomogeneity of the N_O distribution in the bottom part of the single crystal.

The new method provides for a 35–40 % increase in the length of the single crystal portion with the rated N_O (within (8 ± 1) × 10^{17} cm^{-3}) and a radial N_O scatter of ≤ 5 %.

The study showed that the best N_O distribution is achieved for argon gas blowing from 4–7 nozzles and the greatest N_C reduction is attained for argon gas blowing from 6–7 nozzles. One nozzle is sufficient to suppress carbon supply from the growth chamber atmosphere so to make N_C in the single crystal approximately the same as N_C in the charge. Argon gas blowing from 7 nozzles is preferred for achieving N_C that is guaranteed to be lower than that in the charge. Charge with N_C > (0.8–1.0) × 10^{17} cm^{-3} is not suitable for the growth of single crystals for microelectronics applications. Therefore purifying a silicon charge with a lower N_C one can obtain N_C values in the as-grown single crystal that are actually lower than those shown in Table 1 (Variant 3). More thorough carbon purification can be adequate in processes designed for cheaper carbon-containing silicon charge, e.g. growth of multicrystalline silicon ingots for photovoltaic applications.

Design of a similar process for phosphorus-doped silicon requires correcting the master alloy quantity in the charge since phosphorus is a far more volatile impurity and has a much lower K_{eff} than boron. To avoid intense phosphorus evaporation it is recommendable to reduce the number of nozzles to 2–3 or reduce the argon gas flowrate from the nozzles to ~1.2 nl/min. Since phosphorus doping leads to more intense carbon displacement to the liquid phase than for boron doping [40], these corrections to the process will be sufficient for N_C reduction in phosphorus doped silicon single crystals.

Figures 2–4 show N_O distributions in the length and cross-sections of the single crystals and the N_C distribution

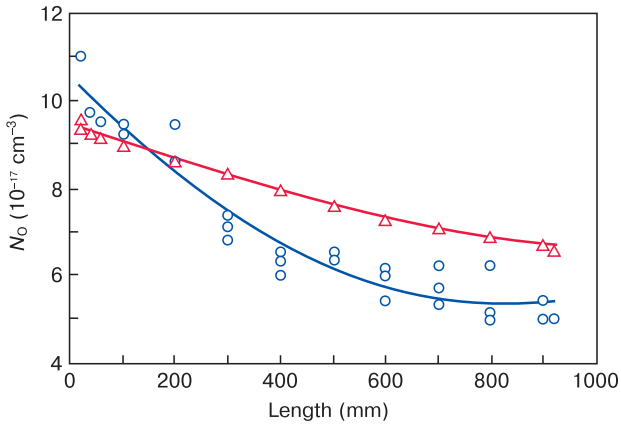

Figure 2. Oxygen concentration distribution along crystal length for (o) conventional and (Δ) designed growth methods. Silicon Grade 1A2yaO$_2$ KDB-10/2.5-102.5, charge weight: 22 kg, measured at the center of section.

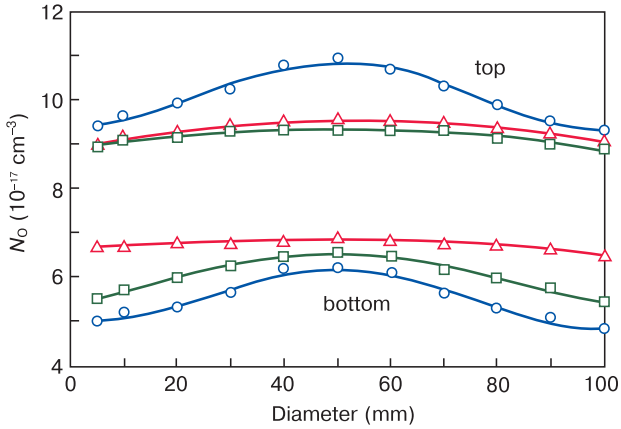

Figure 3. Oxygen distribution in top and bottom cross-sections of single crystals grown with (o) conventional and (Δ) designed methods and (□) with programmable ω_c variation. Silicon Grade 1A2yaO$_2$ KDB-10/2.5, charge weight: 22 kg, section distances from constant crystal diameter establishment point: 20 mm (top) and 800 mm (bottom)

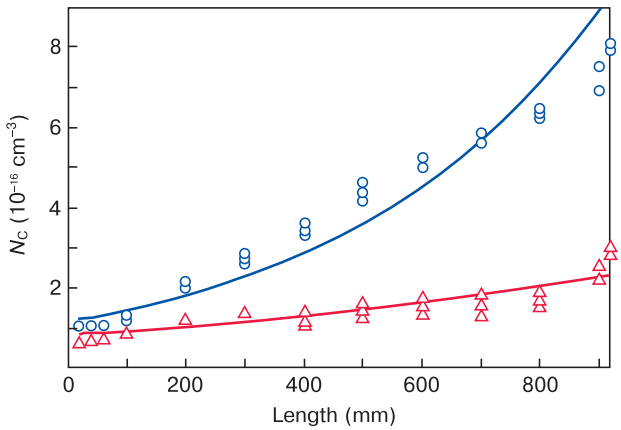

Figure 4. Carbon concentration distribution along crystal length for (o) conventional and (Δ) designed growth methods. Silicon Grade 1A2yaO$_2$ KDB-10/2.5-102.5, charge weight: 22 kg, measured at center of section, carbon concentration in charge: (5–7) · 10^{16} cm^{-3}

in the length of the single crystals for the conventional and the new growth methods (Variants 1 and 3, respectively).

The new growth process improves the homogeneity of the boron microdistribution as shown by 0.01 mm step electrical resistivity measurements. The microinhomogeneity of the oxygen distribution also proved to be lower (Fig. 5). Oxygen distributions were measured with a Bruker IFS-113V Fourier spectrometer for a 1 mm step and a 0.5 mm scanning beam diameter. The microinhomogeneity of the oxygen distribution in the top section of the single crystal was ±20 % for the conventional growth method and ±6 % for the new method, the bottom section results being ±15 % and ±5 %, respectively.

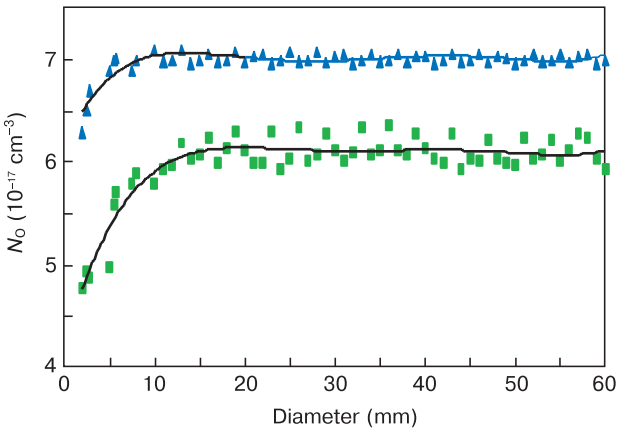

Figure 5. Oxygen microdistribution in cross-sections of silicon single crystals grown (▲) using designed method and (■) with programmable ω_c variation. Silicon Grade 1A2yaO$_2$ KDB-10/2.5-102.5, section distances from constant crystal diameter establishment point: 700 mm, charge weight: 22 kg

Control of natural and forced convective flows in silicon melt can make a sufficient contribution to the distribution of the doping and background impurities in the single crystal. The development of convective flows caused by the variation of the growth rate, thermal convective flows and crystal and crucible rotation speeds during single crystal growth provides for an improvement of single crystal homogeneity but may not be advantageous for achieving the required concentrations and macro/microhomogeneity of doping impurity, oxygen and carbon distributions. Additional melt surface blowing with argon gas flows is an efficient tool for improving the quality of single crystals.

However the problem of controlling the concentration of oxygen supplied to the melt due to silicon melt interaction with the quartz crucible cannot be solved without the use of external energy impacts. Single crystal growth in magnetic fields on conventional commercial equipment [43] reduced the oxygen concentration in the single crystals by 1.5–2.0 times. Still the existing technologies of single crystal growth in magnetic fields do not allow reducing the oxygen concentration to below 4 · 10^{17} cm^{-3} and further N_O reduction will be quite a difficult task without understanding of the actual processes occurring during crystallization and optimization of external controlling

energy impacts. One should further take into account the inter-impurity interactions due to deformation, electrostatic and chemical processes [44], phase transformations in the co-existence range of solid and liquid solid solutions, electromagnetic and gravity-related phenomena accompanying the crystallization, as well as the resistance of the growing crystalline structure to impacts tending to violate the free crystallization process (the Le Chatelier-Brown principle) [45]. The latter resistance shows itself in the following known phenomena:

– predominance of the contribution of crystallographic orientation over normal tangential growth during silicon atom incorporation at the crystallization front [1];
– relief of growth-induced internal elastic stresses due to the formation of regions with looser atomic packing [44];
– stable mechanism of polygonization upon interruption of established growth rate for heavily doped single crystals [47, 48] etc.

The contribution of external controlling energy impacts should be harmonized with system self-organization processes (equilibrium crystallization, phase transitions, changes in electronic structure of neighboring atoms, change of Fermi level position upon impurity introduction) in order for as-grown single crystals to have the required properties [49]. For example, the recently discovered phenomenon of magnetic field generation by rotating oxygen and carbon containing molecules [50] allows one to hypothesize that the concentrations of these atoms may vary during their incorporation into crystals in external magnetic fields and that this process will be controllable.

4. Conclusion

A single crystal silicon growth method that includes additional melt surface blowing with argon gas jets was designed. As-grown single crystals have 35–40 % longer portions with $N_O = (8 \pm 1) \times 10^{17}$ cm^{-3} and radial scatter of $N_O \leq 5$ % as compared with those for conventional Cz-Si single crystals or for single crystals grown at programmable crucible rotation speed.

Additional argon gas blowing reduces N_C in the single crystals to below N_C in the charge.

Single crystals grown using the designed method have higher (by 5–6%) microhomogeneity of doping impurity and oxygen distributions.

Further advance towards a successful technology of highly homogeneous single crystals with guaranteed preset properties will require harmonizing external energy impacts with the atomic energies of the crystallizing material and due allowance for the contribution of system self-organization processes.

References

1. Kritskaya T.V. *Sovremennye tendentsii polucheniya kremniya dlya ustroistv elektroniki* [Current trends in the production of silicon for electronic devices]. Zaporozhye: Izd-vo ZGIA, 2013, 353 p. (In Russ.)
2. Tasit Murki. *Zakon Mura protiv nanomerov* [Moore's law against nanomeres]. (In Russ.). URL: http://subscribe.ru/archive/comp.news.ixbt/201111/02111527.html
3. Mozer A.P. Silicon wafer technology. Status and overlook at the millennium and a decade beyond. *Solid State Phenomena*. 1999; 69–70: 1–12. https://doi.org/10.4028/www.scientific.net/SSP.69-70.1
4. Fistul V.I. *Fizika i materialovedenie poluprovodnikov s glubokimi urovnyami* [Physics and materials science of semiconductors with deep levels]. Moscow: Metallurgiya, 1992, 240 p. (In Russ.)
5. Barraclough K.G. Oxygen in Czochralski silicon for ULSI. *J. Cryst. Growth*. 1990; 99(1–4): 654–664. https://doi.org/10.1016/S0022-0248(08)80002-4
6. Monkowski J.R. Gettering processes for defect control. *Solid State Technology*. 1981; 24(7): 44–51.
7. Petlitsky A.N., Ponomar V.N., Tarasik M.I., Yanchenko A.M. Formation of a reproducible getter in silicon. *Izv. vuzov. Tsvetnaya metallurgiya*. 1987; (5): 50–54. (In Russ.)
8. Petlitsky A.N. *Osobennosti getterirovaniya primesei v kislorodsoderzhashchem kremnii* [Features of the gettering of impurities in oxygen-containing silicon]. Summary Diss. Cand. Sci. (Phys.-Math.). Minsk, 2004, 21 p. (In Russ.)
9. Voronkov V.V., Falster R. Grown-in microdefects, residual vacancies and oxygen precipitation bands in Czochralski silicon. *J. Cryst. Growth*. 1999; 204(4): 464–474. https://doi.org/10.1016/S0022-0248(99)00202-X
10. Ravi K.V. Materials quality and materials cost. Are they on a collision course? *Solid State Phenovena*. 1999; 69–70: 103–110. https://doi.org/10.4028/www.scientific.net/SSP.69-70.103
11. Puzanov N.I., Eidenzon A.M. Selective interaction of twin boundaries with vacancies and self-interstitials in dislocation-free Si tetracrystals. *J. Cryst. Growth*. 1997; 178(4): 459–467. https://doi.org/10.1016/S0022-0248(97)00005-5
12. Dashevskii M.Ya. Osobennosti tekhnologii vyrashchivaniya sovershennykh i odnorodnolegirovannykh monokristallov kremniya [Features of the technology of growing perfect and uniformly doped silicon single crystals]. *Nauchn. shk. mosk. gos. in-ta stali i Splavov: 75 let: Stanovlenie i razvitie*. Moscow: Izd-vo MISiS, 1997: 462–468. (In Russ.)
13. *Tekhnologiya poluprovodnikovogo kremniya* [Technology of semiconductor silicon]. Ed. E.S. Falkevich. Moscow: Metallurgiya, 1992, 408 p. (In Russ.)
14. Mevius V.I., Pulner E.O. Investigation of the flow of silicon melt in a floating crucible. *Tsvetnye metally*. 1985; (9): 56–58. (In Russ.)
15. Tairov Yu.M., Tsvetkov V.F. *Tekhnologiya poluprovodnikovykh i dielektricheskikh materialov* [Technology of semiconductor and dielectric materials]. Moscow: Vysshaya shkola, 1990, 424 p. (In Russ.)
16. Patent 4040895 (USA). Control oxygen in silicon crystals. W.J. Patrick, W.A. Westdorp, 1977.
17. Verezub N.A., Lednev A.K., Myaldun A.Z., Polezhaev V.I., Prostomolotov A.I. Physical modeling of convective processes during

crystal growth by the Czochralski method. *Kristallografiya*. 1999; 44(6): 1125–1131. (In Russ.)
18. Verezub N.A., Zharikov E.V., Myaldun A.Z., Prostomolov A.I. Analysis of the effect of low-frequency vibrations on temperature pulsations in a melt during crystal growth by the Czochralski method. *Kristallografiya*. 1996; 41(2): 354–361. (In Russ.)
19. Lyubalin M.D. Effect of parameters of the process of obtaining semiconductor crystals by the Czochralski method on the temperature of the melt and gas near the crystallization front. *Tsvetnye metally*. 1987; (3): 66–68. (In Russ.)
20. Patent 2077615 (RF). *Sposob vyrashchivaniya monokristallov kremniya* [A method of growing silicon single crystals]. Z.A. Salnik, Yu.A. Miklyaev, 1997.
21. Software for optimization and process development of crystal growth from melt and solution. URL: www.str-soft.com
22. Müller G. Crystal growth from the melt. Convection and heterogeneity. Berlin; Heidelberg: Springer-Verlag, 1988, 138 p.
23. Berdnikov V.S., Vinokurov V.A., Vinokurov V.V., Gaponov V.A. The influence of convective heat transfer regimes in a crucible-melt-crystal system on a shape of the solidification front in Czochralski method. *Teplovye protsessy v tekhnike = Thermal Processes in Engineering*. 2011; 3(4): 177–186. (In Russ.)
24. Shi D. *Chislennye metody v zadachakh teploobmena* [Numerical methods in heat transfer problems]. Moscow: Mir, 1988, 554 p. (In Russ.)
25. Kobeleva S.P., Anfimov I.M., Berdnikov V.S, Kritskaya T.V. Possible causes of electrical resistivity distribution inhomogeneity in Czochralski grown single crystal silicon. *Modern Electronic Materials*. 2019; 5(1): 27–32. https://doi.org/10.3897/j.moem.5.1.46315
26. Gelfgat Yu.M. Rotating magnetic fields as a means to control the hydrodynamics and heat/mass transfer in the processes of bulk single crystal growth. *J. Cryst. Growth*. 1999; 198–199(1): 165–165. https://doi.org/10.1016/S0022-0248(98)01192-0
27. Patent 6156119 (USA). Silicon single crystals and method for producing the same. H. Ryoji, J. Kouichi, O. Tomohiko, 1998.
28. Patent 6113688 (USA). Process for producing single crystal. K. Souroku, J. Makoto, 2000.
29. Tkacheva T.M., Gorin S.O., Laptev A.V. et al. Impurity heterogeneity and structure of dislocation-free silicon single crystals grown by the Czochralski method in a magnetic field. *Svoistva legirovannykh poluprovodnikovykh materialov* [Properties of doped semiconductor materials]. Moscow: Nauka, 1990: 127–131. (In Russ.)
30. Handbook of semiconductor silicon technology. Ed. by W.C.O'Mara, R.B. Herring, L.P. Hunt. Park Ridge (New Jersey): NOYES Publications, 1990, 795 p.
31. Turovskii B.M. The effect of rotation of a crucible with a melt on the oxygen content in silicon crystals grown by the Czochralski method. *Nauchnye trudy Giredmeta* [Scientific works of Giredmet]. Vol. 25. Moscow: Metallurgiya, 1969: 113–116. (In Russ.)
32. Evstratov I.Yu., Kalaev V.V., Nabokov V.N., Zhmakin A.I., Makarov Yu.N., Abramov A.G., Ivanov N.G., Rudinsky E.A., Smirnov E.M., Lowry S.A., Dornberger E., Virbulis J., Tomzig E., Ammon W.V. Global model of Czochralski silicon growth to predict oxygen content and thermal fluctuations at the melt-crystal interface. *Microelectronic Engineering*. 2001; 56(1–2): 139–142. https://doi.org/10.1016/S0167-9317(00)00516-5
33. Kalaev V.V. Combined effect of DC magnetic fields and free surface stresses on the melt flow and crystallization front formation during 400 mm diameter Si Cz crystal growth. *J. Cryst. Growth*. 2007; 303(1): 203–210. https://doi.org/10.1016/j.jcrysgro.2006.11.345
34. Chen J.-C., Guo P.-C., Chang C.-H., Teng Y.-Y., Hsu C., Wang H.-M., Liu C.-C. Numerical simulation of oxygen transport during the Czochralski silicon crystal growth with a cusp magnetic field. *J. Cryst. Growth*. 2014; 401: 888–894. https://doi.org/10.1016/j.jcrysgro.2013.10.040
35. Chartier C.P., Sibley C.B. Czochralski silicon crystal growth at reduced pressures. *Solid State Technology*. 1975; 8(2): 31–33.
36. Application 2548046 (Germany). Verfharen zur Herstellung einkristalliner Siliciumstäbe. Wacker-Chemitronic Ges. für Electronik-Grundstoffe mbit, H. Stock, A. Ellbrunner.
37. Xin Liu, Hirofumi Harada, Yoshiji Miyamura, Xue-feng Han, Satoshi Nakano, Shin-ichi Nishizawa, Koichi Kakimoto. Numerical analyses and experimental validations on transport and control of carbon in Czochralski silicon crystal growth. *J. Cryst. Growth*. 2018; 499: 8–12. https://doi.org/10.1016/j.jcrysgro.2018.07.020
38. Liu X., Nakano S., Kakimoto K. Development of carbon transport and modeling in Czochralski silicon crystal growth. *Cryst. Res. Technol.* 2017; 52(1): 1600221 (11 pp). https://doi.org/10.1002/crat.201600221
39. Torbjörn Carlberg. A quantitative model for carbon incorporation in Czochralski silicon melts. *J. Electrochem. Soc.* 1983; 130(1): 168–171. https://doi.org/10.1149/1.2119648
40. Kritskaya T.V. Properties of silicon single crystals grown by the Czochralski method in controlling flows of surface heat and mass transfer. *Teoriya i praktika metallurgii*. 2005; (4–5): 79–83. (In Russ.)
41. Patent 2076909 (RF). *Sposob vyrashchivaniya monokristallov kremniya* [A method of growing silicon single crystals]. Z.A. Salnik, Yu.A. Miklyaev, 1997.
42. Certificate of Authorship 327429 (USSR). *Sposob polucheniya monokristallov kremniya* [A method of obtaining silicon single crystals] V.E. Bevz, N.N. Danileiko, A.I. Golubov, T.V. Kritskaya, B.L. Shklyar, E.S. Falkevich, 1990.
43. PVA TePla AG Germany. Crystal Growing Systems: Contigo Concept GmbH & Co. URL: www.pvatepla.com
44. Fistul V.I. *Vzaimodeistvie primesei v poluprovodnikakh* [Interaction of impurities in semiconductors]. Moscow: Nauka, 1999, 318 p. (In Russ.)
45. Vasiliev A.V., Baranov A.I. *Defektno-primesnye reaktsii v poluprovodnikakh* [Defective-impurity reactions in semiconductors]. Novosibirsk: Izd-vo SO RAN, 2001, 256 p. (In Russ.)
46. Fritzler K.B. *Formirovanie ogranki i kristallicheskoi struktury kremniya*, *vyrashchennogo metodom bestigel'noi zonnoi plavki* [The formation of the faceting and crystalline structure of silicon grown by the crucibleless zone melting method]. Diss. Cand. Sci. (Phys.-Math.). Novosibirsk, 2012,149 p. (In Russ.)
47. Kritskaya T.V., Golovko O.P. Deformation defect formation during the growth of silicon single crystals by the Czochralski method. Metallurgy. *Proceedings of the Zaporizhzhya State Engineering Academy*. Zaporozhye: ZGIA, 2003; (7): 64–66. (In Russ.)
48. Golovko O.P., Kritskaya T.V., Kutsev M.V. Formation of a polycrystalline region in heavily doped silicon single crystals. *Izvestiya Vysshikh Uchebnykh Zavedenii. Materialy Elektronnoi Tekhniki = Materials of Electronics Engineering*. 2001; (4): 38–40. (In Russ.)
49. Kritskaya T.V., Zhuravlev V.N. Hypothesis of the process of growing single crystals with analytically predicted electrophysical parameters. *Tezisy dokladov mezhdunarodnoi konferentsii «Kremnii-2016» = Abstracts of the International Conference «Silicon-2016»*. Novosibirsk, 2016: 91. (In Russ.)
50. Earth. Chronicles of Life: The rotation of the molecule was first filmed. (In Russ). URL: http://earth-chronicles.ru/news/2019-07-30-130983